

A phosphate-based proton conducting solid electrolyte hydrocarbon gas sensor

Badri K. Narayanan, Sheikh A. Akbar, Prabir K. Dutta*

*Department of Chemistry, Center for Industrial Sensors and Measurements (CISM), The Ohio State University,
120 West 18th Avenue, Columbus, OH 43210, USA*

Received 13 March 2002; received in revised form 23 July 2002; accepted 20 August 2002

Abstract

A potentiometric sensor based on a proton conducting sodium phosphate solid electrolyte was utilized in conjunction with a hydrogenation catalyst to detect methane at 600 °C. By using a two-compartment cell with gold electrodes and H₂ gas, it was established that the solid electrolyte behaves as a proton conducting material, exhibiting Nernstian behavior. For sensing methane, Pt/CeO₂ was painted onto one of the gold electrodes. Two cell designs, including a two-chamber cell with a reference gas, as well as a planar cell without a reference gas were examined for methane sensing. Pt/CeO₂ prepared with colloidal Pt tested on the planar cell showed superior sensitivity to methane. A mixed potential behavior, arising from the combined effect of electrochemical reactions of methane and its oxidation products is proposed to give rise to the methane response.

© 2002 Elsevier Science B.V. All rights reserved.

Keywords: Methane sensor; Hydrogen sensor; Methane oxidation; CO interference

1. Introduction

Environmental pollution has resulted in stringent regulations to further reduce combustion emissions. The control of fuel efficiency and monitoring emissions has become a very important issue for the automotive industry and a challenging prospect for gas sensor development to meet the requirements of the industry. The Environmental Protection Agency (EPA) has regulated the emission of hydrocarbon gases and has made it mandatory for all automotive manufacturers to drop the threshold from 0.25 g/mile non-methane hydrocarbons (NMHCs) in 1996 to 0.12 g/mile NMHCs in 2004 [1–3].

Presently, in automobiles, there is a complex feedback system associated with the oxygen sensors to control the air/fuel ratio. It is apparent that any additional information obtained about the emissions will be of great help in optimizing the combustion process. There is also a need to monitor the amount of hydrocarbons that evaporate when the engine is idle. Since the early 1970s, the federal standards for the evaporative emission control have been continuously reinforced.

The petroleum and the chemical industry utilize conventional electro-catalytic hydrocarbon gas detectors. Catalytic

poisoning, interference from other combustible gases and limited operating temperature range are some of the limitations associated with these sensors. The infrared hydrocarbon detectors provide the best sensitivity and selectivity to hydrocarbon gases, but the high cost of the equipment, the need for reference sampling gas and the difficulty in miniaturizing makes it difficult to use it for online monitoring.

Proton conducting ceramics have been suggested to have potential for sensing hydrocarbons [4]. Indium-doped calcium zirconate has been known to show good proton conductivity and potential for hydrocarbon gas sensing [5]. Most proton conductors reported in literature are complex oxides operating at temperatures as high as 1000 °C. These proton conducting ceramics are predominantly perovskite-based, such as the cerates and zirconates of barium and strontium [6]. Some pyrochlore structure-based materials, such as La₂Zr₂O₇, have also been known to show good proton conductivity [7]. The proton conductive behavior of these ceramics is a function of the oxygen vacancy concentration and hence shows dependence on oxygen partial pressure.

Another class of materials reported in literature with high proton mobility are the oxyacid salts [8]. Lithium sulfate has been reported to show high proton conductivity and has been suggested for fuel cell applications at 600 °C [9]. The alkali orthophosphates have also been reported to have potential

* Corresponding author. Tel.: +1-614-2924532; fax: +1-614-6885402.
E-mail address: dutta.1@osu.edu (P.K. Dutta).

for fuel cell and gas sensing applications [10]. Sodium orthophosphate, Na_3PO_4 , is a versatile host structure for solid solution formation. The high temperature cubic phase can be stabilized to room temperature by doping with aliovalent ions, such as Al [11].

The cubic phases of these alkali phosphates, nitrates and sulfates are of interest as potential proton conductors. The SO_4 and PO_4 groups in these face-centered cubic lattices have a high degree of rotational freedom that aids in the mobility of protons. Protons attach themselves to these tetrahedral groups at the vertices of the cubic structure and move from one tetrahedron to the other. This mechanism is referred to as the “cog-wheel” or “paddle wheel” mechanism [12,13]. For the phosphate compounds, proton conductivity up to 0.006 S/cm at 600 °C has been reported [14]. Using proton conducting zirconium phosphates, Alberti et al. have developed hydrocarbon gas sensors [15].

The results reported in this paper deals with the design of a hydrocarbon gas sensor involving an oxyacid-based electrolyte material in conjunction with a hydrogenation catalyst.

2. Experimental

2.1. Preparation of aluminum-doped sodium phosphate ($\text{Na}_{3(1-x)}\text{Al}_x\text{PO}_4$)

Sodium and aluminum phosphates were anhydrous commercial grade with 99% purity obtained from Alfa Aesar. An amount of 11.48 g of sodium phosphate was added to 3.66 g of aluminum phosphate and ball milled in acetone for 6 h. The solvent was removed at room temperature. The powder was then dried and calcined at 1000 °C. Pellets were pressed in a hydraulic press and the green pellets were sintered at 1050 °C for 12 h. Powder X-ray diffraction (XRD) was used for phase identification. The spectra was collected at 5°/min between 20 and 60° with a Scintag Pad V diffractometer, using $\text{Cu K}\alpha$ radiation at 45 kV and 20 mA current.

2.2. Preparation of 1% Pt/CeO₂ catalyst

Two sources of Pt were used. The first was just Pt ink. The second was Pt in colloidal form [16]. An amount of 25 ml of 2% aqueous solution of PVA was added to 11 ml of H_2O . Then 2 ml of K_2PtCl_4 solution (0.5%) was added. To this solution 0.8 ml of 4% NaOH was added. NaBH_4 was used to reduce Pt^{2+} to metallic Pt. For 19 mg of K_2PtCl_4 , 4 mg of NaBH_4 was added. The mixture was stirred vigorously upon which the colloidal Pt formed. CeO_2 was added to the Pt to obtain the final catalyst.

2.3. Sensor design

2.3.1. Two-chamber hydrogen gas sensor

A two-chamber hydrogen gas sensor was designed to establish the proton conductive behavior of the electrolyte

material. A hydrogen concentration cell was set-up by sealing a pellet of the electrolyte material on top of an alumina tube. A glass-based inorganic sealing material, known as material K, developed by Argonne National Laboratory, was used. The cell is depicted in Fig. 1a. The concentration cell can be represented as:



The hydrogen concentration in the reference side was maintained at 500 ppm in a background of N_2 . Hydrogen concentration on the sensing side was increased in steps, as outlined below.

2.3.2. Two-chamber hydrocarbon gas sensor

A two-chamber hydrocarbon gas sensor similar to the hydrogen concentration cell was designed to establish the sensitivity of the overlayer–electrolyte combination to the presence of hydrocarbons. Methane (in N_2) was chosen as the sensing gas. In the reference side, the gas was nitrogen. The electrolyte material was aluminum-doped sodium phosphate and the Pt/CeO₂ was applied in the form of an overlayer over the gold electrode on the sensing side of the cell.

2.3.3. Planar hydrocarbon gas sensor

A planar sensor was designed using a sintered pellet of the electrolyte. Gold electrodes were painted on the pellet adjacent to each other, as shown in Fig. 1b. One of the electrodes was coated with an overlayer of Pt/CeO₂.

2.4. Electrical measurements and gas sensitivity studies

Gold electrodes were painted and gold lead wires (0.25 mm diameter obtained from Alfa Aesar) were attached using Heraeus gold ink at room temperature. The assembly was cured by raising the temperature to 800 °C at a rate of 2 °C/min and keeping at the curing temperature for 1 h before cooling it to room temperature slowly.

The gas sensitivity studies were conducted inside a Lindberg furnace as a function of gas concentration and temperature. Nitrogen was used as the background gas. Gas flow rates and concentrations were controlled by mass flow meters (Sierra 840L). The sensing gas was introduced in steps and the sensitivity was established by correlating the voltage (emf) increase with increase in the gas concentration. The emf response of the sensor was recorded using a HP 34401 multimeter and a Benchlink data acquisition software.

3. Results and discussion

3.1. Electrolyte preparation

The cubic phase, which is the proton conducting phase of sodium phosphate was stabilized by the addition of 0.3 mol aluminum phosphate. Powder XRD diffraction

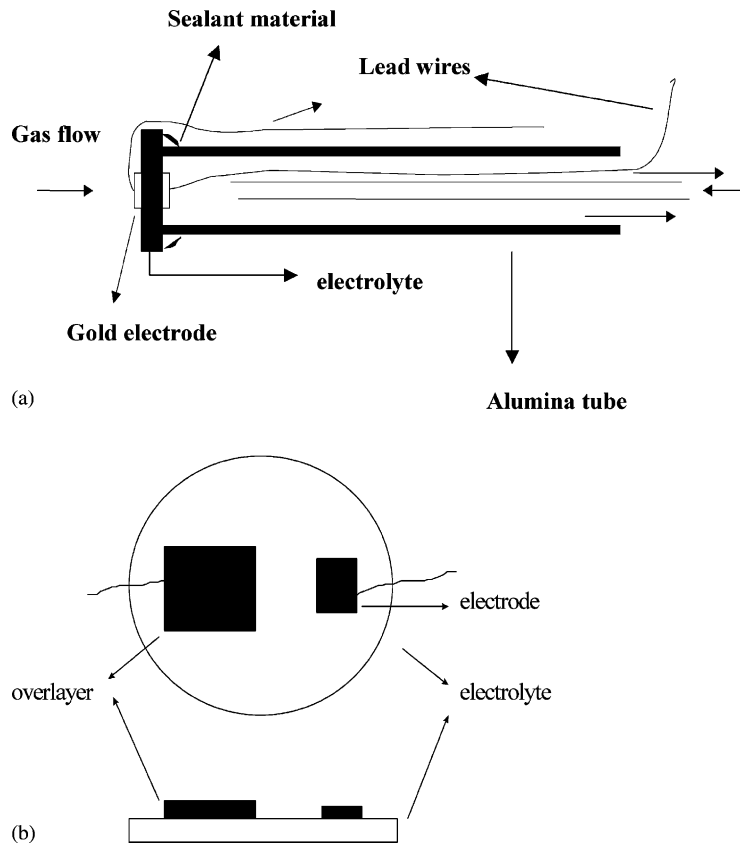


Fig. 1. Schematic representation of: (a) a two-chamber sensor; (b) a planar sensor.

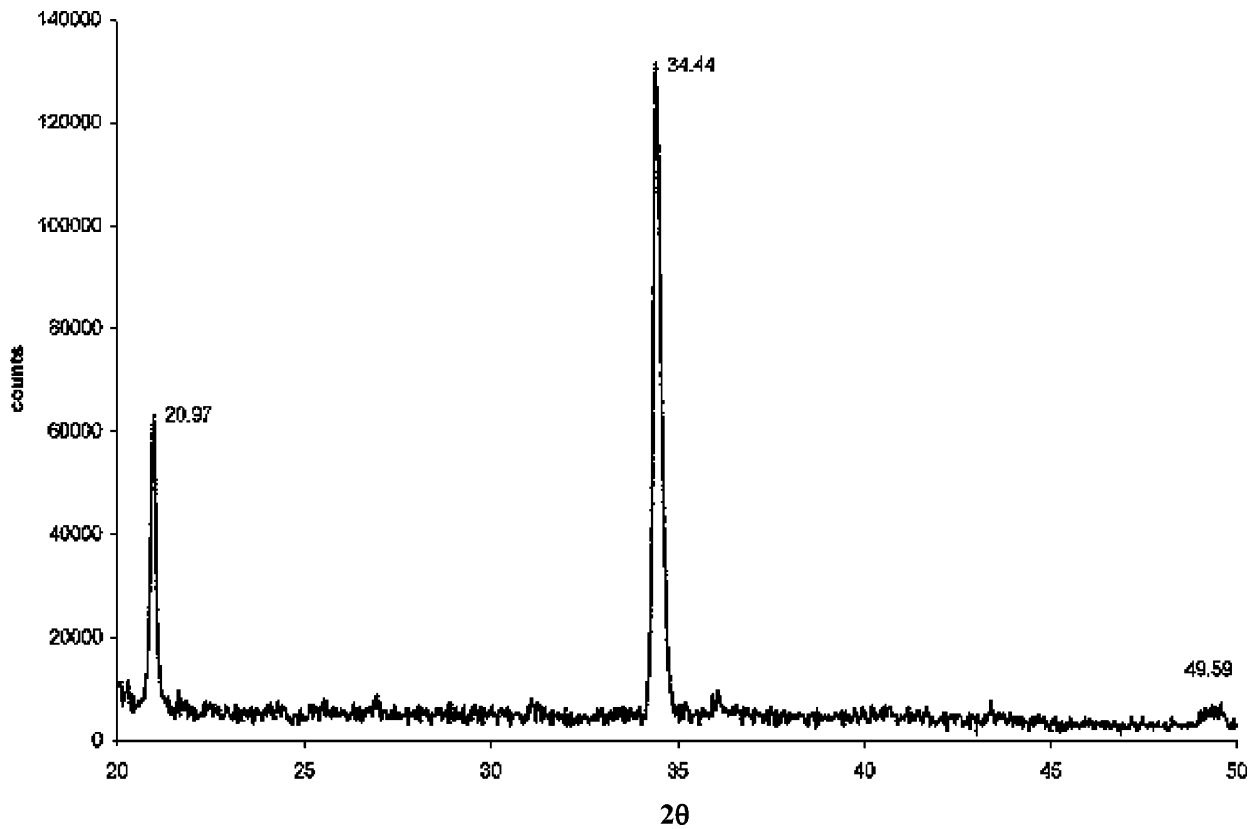


Fig. 2. X-ray diffraction pattern of the cubic phase stabilized by 0.3 mol aluminum addition in sodium phosphate.

results confirm the stabilization of the cubic phase at room temperature (Fig. 2). The absence of any extraneous peak in the diffraction pattern also indicates the formation of a single phase.

3.2. Conducting properties of electrolyte

A two-chamber hydrogen sensor (Fig. 1a) was fabricated and the sensitivity to hydrogen was examined. Response of the cell at 600 °C to changes in hydrogen concentration is shown in Fig. 3a. A semi-log plot of hydrogen concentration to the open-circuit voltage results in a straight line (Fig. 3b). The open-circuit voltage is a function of the ratio of hydrogen partial pressures on the two sides of the electrolyte and is given by the Nernst equation:

$$\text{emf (V)} = \left(\frac{RT}{nF}\right) \ln\left(\frac{[\text{H}_2]_{\text{I}}}{[\text{H}_2]_{\text{II}}}\right)$$

If the electrolyte material functions by pure proton conduction, the slope should be 34 mV at 600 °C. The slope of the semi-log plot of emf versus $\ln[\text{H}_2^{(\text{I})}/\text{H}_2^{(\text{II})}]$ for a series of experiments was found to be between 28 and 39 mV, with an average value of 35 mV. So, it is reasonable to assume that the electrolyte material is predominantly protonic in nature.

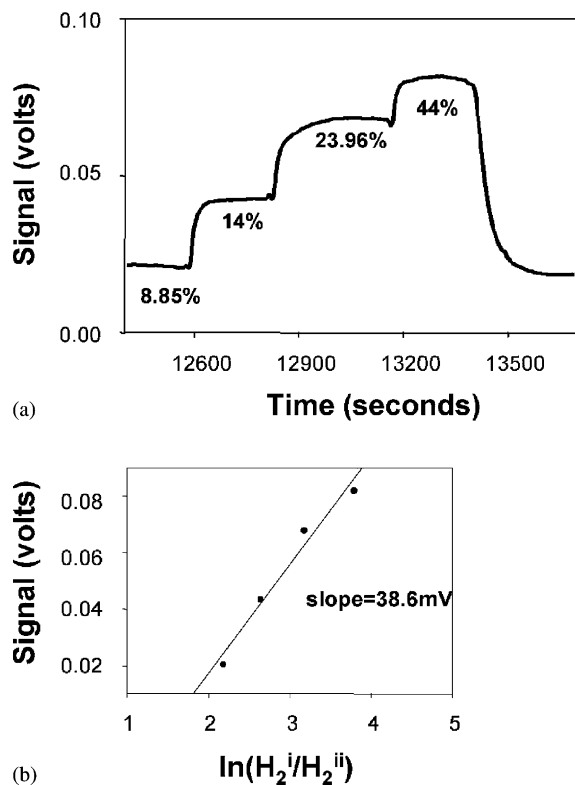


Fig. 3. (a) Response of a two-chamber sensor to changes in hydrogen concentration with a fixed reference of 500 ppm of H_2 at 600 °C. (b) The plot of emf vs. $\log[\text{H}_2]$ demonstrating the Nernstian behavior of the electrolyte material to changing hydrogen concentrations.

3.3. Response to methane gas

Two cell designs were examined for response in the presence of methane. In both cases, only one of the electrodes was covered with Pt/CeO₂. Fig. 4 shows the change in the response of the two-chamber sensor (Fig. 1a) upon exposure of the sensing side to various concentrations of methane, the background gas as well as the reference gas being N₂.

A planar cell, where both the electrodes are exposed to the same gas stream (Fig. 1b) with one of the electrodes covered by Pt/CeO₂ was studied. Two formulations of the overlayer were examined in this cell geometry. Sample A was a mixture of Pt ink and cerium oxide applied as acetone slurry on one of the Au electrodes. Sample B was cerium oxide mixed with a 1% loading of colloidal platinum, synthesized as described in Section 2.2. The response of the sensor with the two different overlayers is compared in Fig. 5. The methane sensitivity improved for the overlayer B. The transient response was also seen to be much better for the 1% Pt/CeO₂ overlayer prepared from colloidal platinum. Fig. 6 shows the response of planar sensors over a wide range of methane concentrations. Four sensors prepared at various times were tested and provides an idea of the variability in sample preparation. It is seen clearly that the response of the sensor does not have a linear dependence on $\log[\text{CH}_4]$. Rather, the fit to the data over the whole concentration range suggests that there are two distinct regions of the semi-log plot.

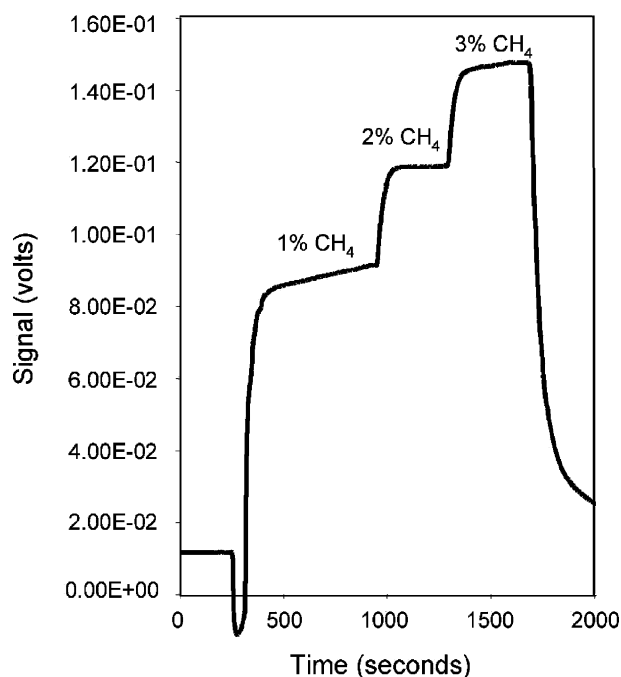


Fig. 4. Performance of the two-chamber sensor to methane at 600 °C, with background of N₂ as the background and reference gas.

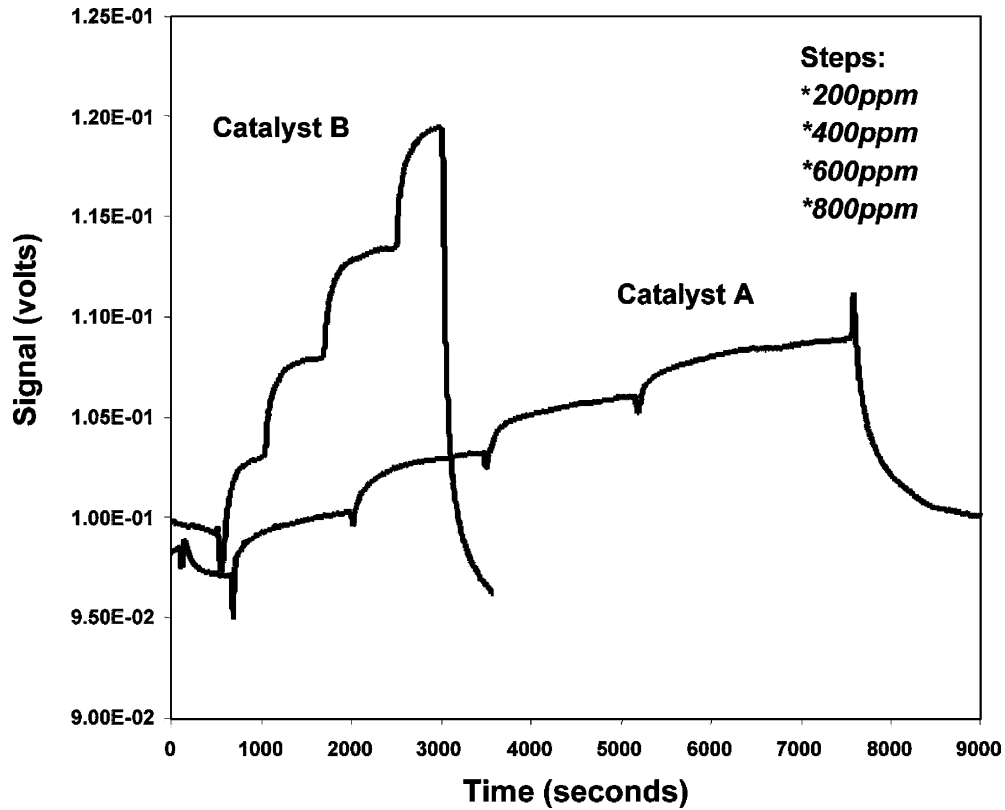


Fig. 5. Performance of the planar sensor with two preparations of Pt/CeO₂ catalysts (A and B) for the sensing of methane in N₂ at 600 °C.

3.4. Sensing mechanism

Pt/CeO₂ is known to be a good catalyst for the partial oxidation of methane to CO and H₂ [17], and was chosen as the overlayer on the sensing electrode for this purpose. Pt acts as a catalyst for H₂ and CO release and the support cerium oxide is responsible for methane activation. Upon complete conversion, each mole of methane introduced

would produce 2 mol of hydrogen. In the present case, since methane is in a N₂ stream, oxidation is occurring by reaction with the ceria support. Trace levels of O₂ in the stream can also aid in the oxidation. The simplest mechanism would involve production of H₂ via methane oxidation without any direct methane redox reactions at the electrode–electrolyte interface. In this case, the response would be entirely dependent on the difference in the hydrogen partial pressures

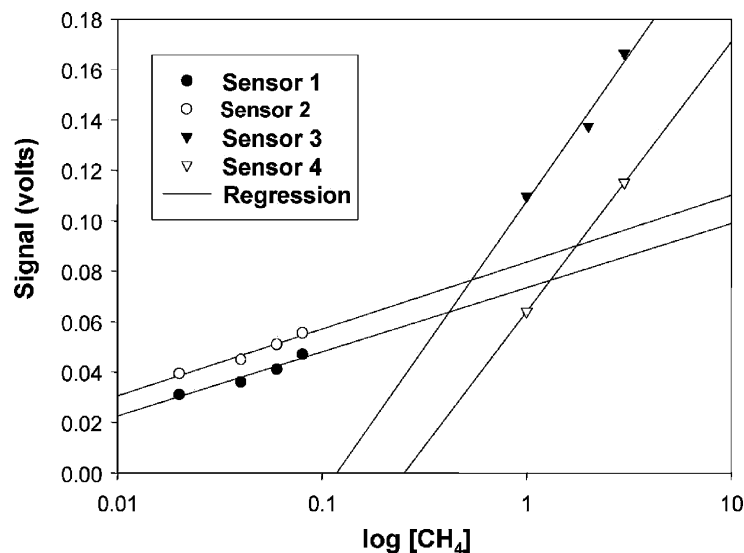


Fig. 6. Plot of response for planar sensors to methane concentrations (four sensors were tested over a range of methane concentrations).

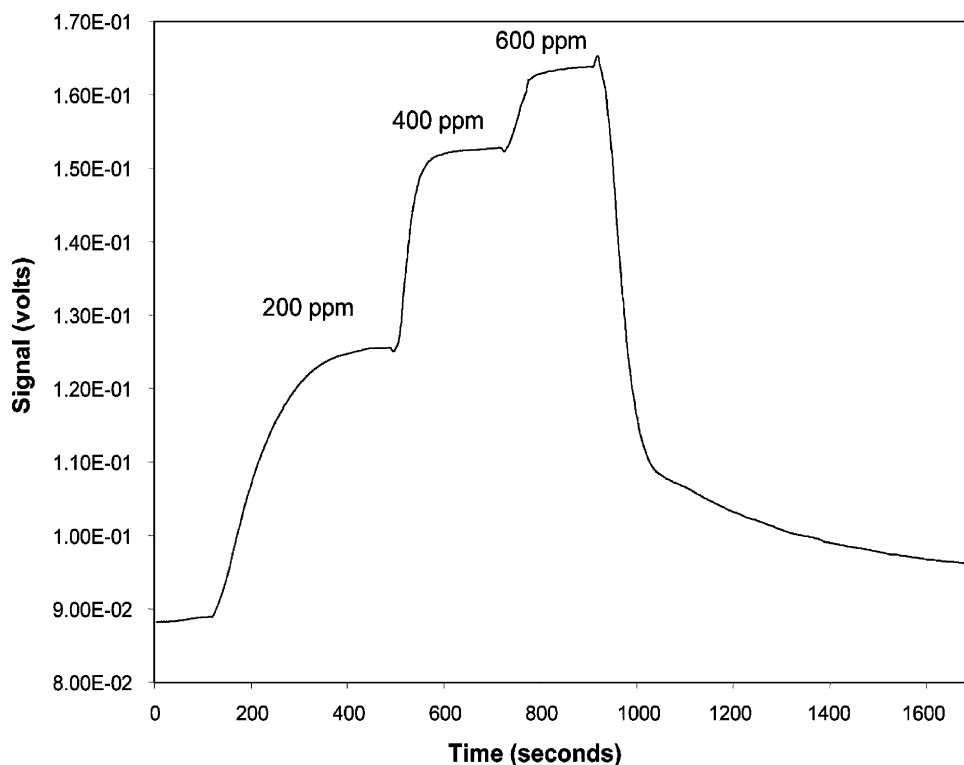


Fig. 7. Response of the two-chamber sensor to CO and H₂ at 600 °C with the same concentration of hydrogen in the sensing and reference sides.

between the sensing and the reference sides. However, the large emf changes with methane concentration variation is supportive of a mixed potential mechanism, since the amount of H₂ produced from the complete oxidation of methane alone would not produce such large signals (e.g. 100 mV in Fig. 4 with 3% methane).

The sensor response to mixtures of CO and H₂ was also examined in the two-chamber cell (Fig. 1a) to evaluate the contribution of the oxidation products of methane to the sensor signal. Fig. 7 shows the response obtained with the two-chamber sensor to a mixture of CO and H₂ (in N₂) on the sensing side and H₂ (N₂) on the reference side. The response of the sensor changes significantly with change in CO concentration even though the hydrogen concentration was maintained the same at both the sensing and reference electrodes. This indicates that a mixture of CO and H₂ is causing a change in the potential of the sensing electrode. These results suggest that the methane and its oxidation products can be engaged directly in electrochemical reactions at the electrode surfaces. Possible electrochemical reactions involving CH₄, CO and H₂ could involve the formation of higher hydrocarbons, methanol or formate at the Au-catalyst–electrolyte interface, and is the focus of future research.

4. Conclusions

Sensors using a sodium phosphate-based proton conducting electrolyte exhibit a potential change upon exposure to

methane. The cubic phase of the electrolyte was stabilized to room temperature by doping with aluminum phosphate. The Nernstian response of the sensor to changes in hydrogen concentration was demonstrated with a slope close to the theoretical value of 34 mV. A Pt/CeO₂ overlayer prepared with colloidal Pt form showed superior sensitivity to methane in planar sensor arrangement. A mixed potential response, arising from the combined effect of electrochemical reactions involving methane and the products of its oxidation at the sensing electrode is proposed.

Acknowledgements

This work was supported by the National Science Foundation grant, EEC-9523358, with matching support from the Edison Materials Technology Center (EMTEC) of the State of Ohio.

References

- [1] E.W. Kaiser, W.G. Rothschild, G.A. Lavoie, The effect of fuel and operating variables on hydrocarbon species distributions in the exhaust from multicylinder engine, *Combust. Sci. Technol.* 32 (1983) 245.
- [2] E.W. Kaiser, W.O. Seigl, Y.I. Hening, R.W. Anderson, F.H. Trinker, Effect of fuel structure on emissions from a spark-ignited engine, *Environ. Sci. Technol.* 25 (1991) 2005.
- [3] T.Y. Chang, D.P. Chock, R.H. Hammerle, S.M. Japar, I.T. Salmeen, Urban and regional ozone air quality: issues relevant to the automobile industry, *Crit. Rev. Environ. Control* 22 (1992) 27.

- [4] K.D. Kreuer, On the development of proton conducting materials for technological applications, *Solid State Ionics* 97 (1997) 1.
- [5] H. Matsumoto, K. Takeuchi, H. Iwahara, Electromotive force of hydrogen isotope cell with a high temperature proton conducting solid electrolyte $\text{CaZr}_{0.9}\text{In}_{0.1}\text{O}_{3-x}$, *J. Electrochem. Soc.* 146 (1999) 1486.
- [6] H. Iwahara, Proton conducting ceramics and their applications, *Solid State Ionics* 86–88 (1996) 9.
- [7] T. Omata, K. Okuda, S. Tsugimoto, S. Otsuka-Matsuo-Yao, Water and hydrogen evolution properties and proton conducting behaviors of Ca^{2+} -doped $\text{La}_2\text{Zr}_2\text{O}_7$ with a pyrochlore structure, *Solid State Ionics* 104 (1997) 249.
- [8] B. Zhu, B.-E. Mellander, Proton conduction in salt–ceramic composite systems, *Solid State Ionics* 77 (1995) 244.
- [9] B. Zhu, B.-E. Mellander, Proton conduction and diffusion in Li_2SO_4 , *Solid State Ionics* 97 (1997) 535.
- [10] B. Zhu, B.-E. Mellander, Intermediate temperature fuel cells with electrolytes based on oxyacid salts, *J. Power Sources* 52 (1994) 289.
- [11] A. Hooper, P. Mcgeehin, K.T. Harrison, B.C. Tofield, *J. Solid State Chem.* 24 (1978) 265.
- [12] A. Kvist, A. Bengtzelius, in: W. van Gool (Ed.), *Fast Ion Transport in Solids*, North-Holland, Amsterdam, 1973, p. 193.
- [13] L. Nilsson, B.C. Tofield, J.O. Thomas, *J. Phys. C* 13 (1980) 6441.
- [14] A. Kvist, A. Lunden, *Z. Naturforsch. A* 20 (1965) 235.
- [15] G. Alberti, A. Carbone, R. Palombari, Solid state potentiometric sensor at medium temperature (150–300 °C) for detecting oxidable gaseous species in air, *Sens. Actuators* 75 (2001) 125.
- [16] L. Rampino, F.F. Nord, Preparation of palladium and platinum synthetic high polymer catalysts and the relationship between particle size and rate of hydrogenation, *J. Am. Chem. Soc.* 63 (1941) 2745.
- [17] K. Otsuka, Y. Wang, E. Sunada, I. Yamanaka, Direct partial oxidation of methane to synthesis gas by cerium oxide, *J. Catal.* 175 (1998) 152.